Novel non-destructive evaluation technique for the detection of poor dispersion of carbon nanotubes in nanocomposites

Antonio Pantano[1,2,*], Nicola Montinaro[1], Donatella Cerniglia[1], Federico Micciulla[2], Silvia Bistarelli[2],

Antonino Cataldo[2], Stefano Bellucci[2],

[1] Dipartimento dell'Innovazione Digitale e Industriale, Università degli Studi di Palermo, 90128,

  Palermo, Italy

[2] INFN-Laboratori Nazionali di Frascati, Via E. Fermi 40, 00044, Frascati, Italy

[3] Dipartimento di Neuroscienze, Imaging e Scienze Cliniche, Università degli Studi di Chieti e Pescara

"G. D'Annunzio" via dei Vestini 31, Chieti, Italy

Abstract

   A wide use of advanced carbon nanotube polymer composites can be boosted by new non-destructive evaluation (NDE) techniques that can test the quality of the products to ensure that their specifications are met. It is well known in literature that the parameter that far more than others can affect the enhancing capabilities of the carbon nanotubes is their dispersion. Here we have presented a novel NDE technique based on infrared thermography able to evaluate the dispersion of the added nanoparticles in polymer nanocomposites. The NDE technique was used to compare pairs of samples whose difference is represented only by the level of dispersion. It was found a significant difference in the thermal response to heat transfer transients. Thus, the thermal response of a nanocomposite allows one to identify consistently good levels of dispersion with respect to lower levels of dispersion. A

reference product, which has the expected dispersion level and achieves the desired design performance, can be used to test the thermal behaviour of other products coming out of the production process and those with poor dispersion can be identified. The physical phenomena that can explain the effects of multi-walled carbon nanotubes (MWCNTs) dispersion on the thermal response of the nanocomposites to the heat transfer transients were also identified.

1. Introduction

In the last decades carbon nanotubes (CNTs) have attracted the interest of the international scientific community because of their exceptional mechanical properties, high thermal conductivity and peculiar electronic properties (ballistic transport). The sp^2 carbon-carbon bond in the basal plane of graphene is the stiffest and strongest in nature. CNTs possess an ideal arrangement of these bonds in their cylindrical and nearly defect-free structures, and hence approach the maximum theoretical tensile stiffness and strength. CNTs also have a 20-30% elastic limit of the strain before failure and a very low density of about 1.75 g/cm^3.

One way to take advantage of the marvellous properties of the CNTs consists in incorporating them into a matrix to build composite materials. The best candidates for this task are undoubtedly polymers, which thanks to their strength, toughness, low weight, and easy processing have been used in a broad variety of industrial applications. The extraordinary mechanical properties, together with high ratios (100-10000) of geometric aspect, stiffness-to-weight, and strength-to-weight, all point to CNTs as potentially ideal reinforcing agents in advanced composites [e.g., 1-9]. However, not only the mechanical properties of the polymer can be improved by adding CNTs, also thermal properties [e.g., 10-14], electrical conductivities [e.g., 15-18] and optical properties [e.g., 19-22] of formed composites can be enhanced. As few examples of applications of CNTs enriched polymer composites we can

mention: aerospace structures, sporting goods, automotive components, medical devices, optical barriers, photovoltaic devices, conducting plastics, materials with high electrostatic dissipation, electromagnetic interference shielding, electrostatic painting of plastics, plastics with high thermal dissipation, biomaterials, strain sensors, damage sensing, gas sensors, optoelectronics, and electromechanical actuation.

This interesting potential has attracted the attention of both industry and academia that have committed to this research field an impressive amount of work, as the very high number of publications shows. However, before seeing an extensive use of CNTs enhanced polymer composites there are a few difficult challenges that need to be addressed. One of them is to develop NDE techniques able to check the quality of the products made of these nanocomposites, in order to guarantee that their specifications are met. The parameter that much more than others can affect the enhancing capabilities of the added nanoparticles is dispersion. All the resulting physical properties of the CNTs based polymer composites depend strongly on the level of dispersion of the CNTs throughout the matrix: homogeneous distribution optimizes the performances, while poor dispersion and formation of bundles always limit the improvement of the properties with respect to the neat polymer.

A possible strategy to tackle the unresolved problems in controlling the dispersion of the nanoparticle filler and the corresponding influence on the properties of the final nanocomposite materials was presented in [23], where rheological methods were applied for controlling the quality of the graphene dispersion. Moreover, it was shown recently that ultrasonic methods are excellent tools for studying nanoparticle distribution over the material bulk and for revealing probable nonuniformity [24]. The NDE technique based on the impulse acoustic microscopy method was applied to observe the bulk microstructure and to measure sonic velocities and elastic moduli in carbon nanocomposite specimens prepared by a traditional method and with the use of a vacuum mixer [25]. However, this

NDE technique is quite slow and allows one to scan only relatively small samples, thus posing strict limits in view of possible industrial applications.

Here we present a novel NDE technique based on infrared thermography able to test the dispersion of the added nanoparticles in nanocomposites. Two different procedures were selected to prepare epoxy nanocomposites with dissimilar degree of nanoparticle dispersion, then several specimens with various volume fractions and diameter ranges of CNTs were manufactured. The novel NDE technique was used to compare pairs of specimens whose only difference was represented by the dispersion levels.

2. Experimental Methods

2.1 Materials

In this study we tested nanocomposite materials made of epoxy resin (Epikote 828, a medium viscosity resin generously provided by Hexion Inc.) loaded with commercial multi-wall carbon nanotubes (MWCNTs), bought from Heji inc. company. The MWCNTs have two different diameter ranges: 8-15 nm and 30-50 nm. In both cases the length ranges between 0.5 micron and 200 micron. Figure 1 shows SEM images of the commercial MWCNTs used as fillers
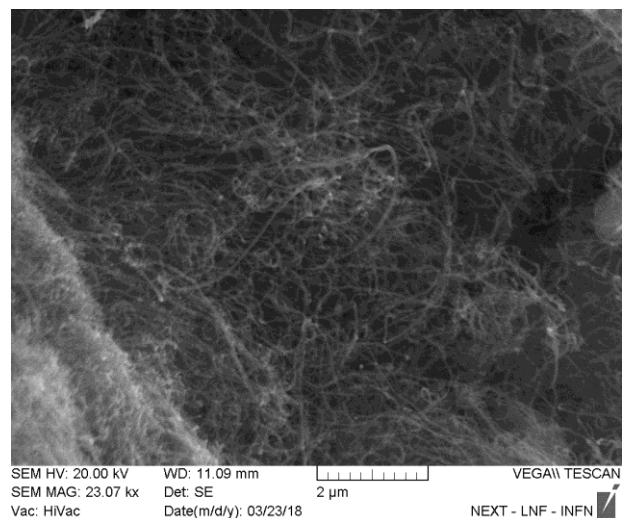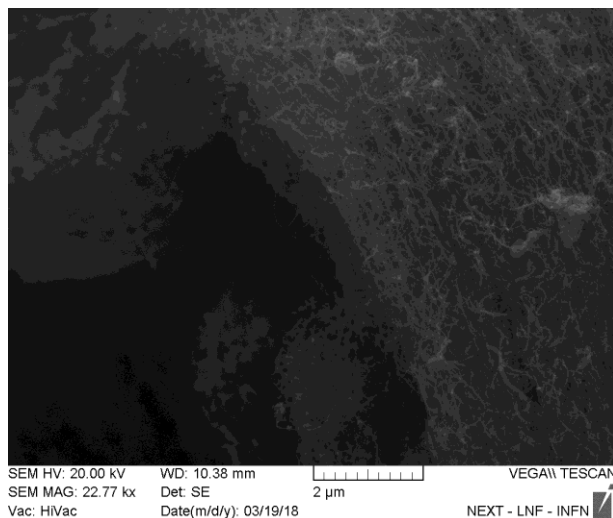
Figure 1. SEM images of the commercial MWCNTs used as fillers: in the left panel, nanotubes with diameters in the range 8-15 nm, in the right panel, nanotubes with diameters in the range 30-50 nm.

In order to understand the results of our work it is important to discuss the difference in thermal conductivity between individual MWCNTs and MWCNTs bundles. Theoretical predictions yield an extremely high thermal conductivity for individual single-wall carbon nanotubes (SWNTs), $\kappa = 6600$ W m^{-1} K^{-1} [26]. Several experiments [27-29] have demonstrated that the thermal conductivity of individual MWCNTs is much lower, $\kappa_{MWCNT} = 600 \pm 100$ W m^{-1} K^{-1}, than theoretically predicted. Moreover, it was proved experimentally [27-29] that coupling within MWCNT bundles further decreases this thermal conductivity to 150 ± 15 W m^{-1} K^{-1}. The reason is that quenching of phonon modes in bundles, reinforced by radial deformation of CNTs by van der Waals forces, substantially reduces the transport abilities inherent for individual CNTs [27]. Table 1 summarizes the thermal properties of individual MWCNTs, MWCNTs in bundle and EPOXY.

Table 1. Thermal properties of individual MWCNTs, MWCNTs in bundle and EPOXY

	MWCNT single	MWCNTs in bundle	EPOXY
Thermal Conductivity [W/m K]	600±100 [27-29]	150 [27-29]	0.35
Specific heat capacity [J/Kg K]	500 [28]	750 [28]	1000

2.2 Processing

The CNTs were used as filler in epoxy resin cured with a curing agent called A1 (a modified TEPA) prepared in our laboratory [30-33]. We tested two different procedures to prepare nanocomposite materials, with the aim to compare the degree of particle dispersion. In fact, the two procedures differ on the mixing method of the two phases. So, the differences, appreciated in the experiments, are due

only to the different dispersion of nanotube. The first procedure is a "by-hand mixing", identified in the following paragraphs by the word HANDS, requiring different steps [34-37], described as follows: first of all, we carry out a vacuum degassing of the liquid epoxy resin for 24h at a pressure of 1-3 millibars. The day after treating epoxy under vacuum, the preparation of the nanofiller suspension begins. The CNTs powders are added to isopropyl alcohol and then sonication in ultrasonic bath for 1.5 hour is carried out to obtain a good dispersion. The so obtained dispersion is mixed with the liquid epoxy resin, the alcohol is entirely evaporated at 150 °C and subsequently the solution is sonicated again for 1.5 hour to disperse the filler in the resin. The curing agent A1 is added to the mixture and followed by hand-mixing for 7 min. The process ends with curing the suspension for 4 hours in an oven at 40°C, followed by 20h in air at normal conditions and finally 4 hours in an oven at 80 °C.

The second procedure is an "automatic mixing" and requires the use of a vacuum planetary centrifugal mixer ARV-310 (Thinky Corporation, Tokyo, Japan), identified in the following paragraphs by the word THINKY. In this planetary mixer the rotation and revolution movement under vacuum pressure reduction enables the simultaneous dispersion of materials and the elimination of submicron-level air bubbles. For this reason, the first step of 24 hours of degassing in the manual preparation is eliminated. By the combination of rotation and revolution, the resin container has a rotation axis at 45°angle whilst it revolves in a set radius, which produces the planetary mixing action. The intensive circulation of the material within the vessel (under 400G of force) results in a quick and thorough mixture along with air being vacuumed out of the container. The revolution speed is adjustable in a range of 200-2000 rpm and the ratio of the revolution speed to the rotation speed of the cup holder is fixed at a 2:1 ratio. The ARV-310 holds up to 310 g of material and the maximum material mixing volume is 250 ml in the vacuum state and 300 ml in the air state [38]. The new procedure requires the following steps. The liquid pre-cured epoxy resin is vacuum degassed for 8 minutes in Thinky, continuously increasing the revolutions per minute up to 2000rpm at 0.2 kPa. After that, the nanofillers

are added directly in epoxy resin and dispersed using an ultrasonic tip at 40% power for 10 minutes. The solution is degassed and mixed for 16 minutes in Thinky at 0.2 kPa. The curing agent A1 is added to the mixture and degassed and mixed for 7 minutes in Thinky at 30 kPa; The mixture is finally cured for 4 hours in an oven at 40°C, 20h in air at normal conditions and 4 hours in an oven at 80 °C.

Earlier [25], the impulse acoustic microscopy technique made it possible to visualize a non-uniform distribution of carbon nanofillers over the specimen bulk, thus demonstrating a reduction of the air content and an enhancement of elastic properties, observed when employing the THINKY vacuum mixing technology in the nanocomposite fabrication.

The specimens produced had the following dimensions: 50 mm overall length, 20 mm width and 5 mm thickness. Four types of nanocomposites, characterized by volume fraction and diameter range of MWCNTs, were manufactured: 5 wt.% and 8-15 nm diameter range, 10 wt.% and 8-15 nm diameter range, 5 wt.% and 30-50 nm diameter range, 10 wt.% and 30-50 nm diameter range. Several specimens of each type, produced both with the first procedure and the second one, were used in the work.

2.3 Material testing

To evaluate the differences in the thermal response of the samples the thermographic experimental setup of Figure 2 is proposed.
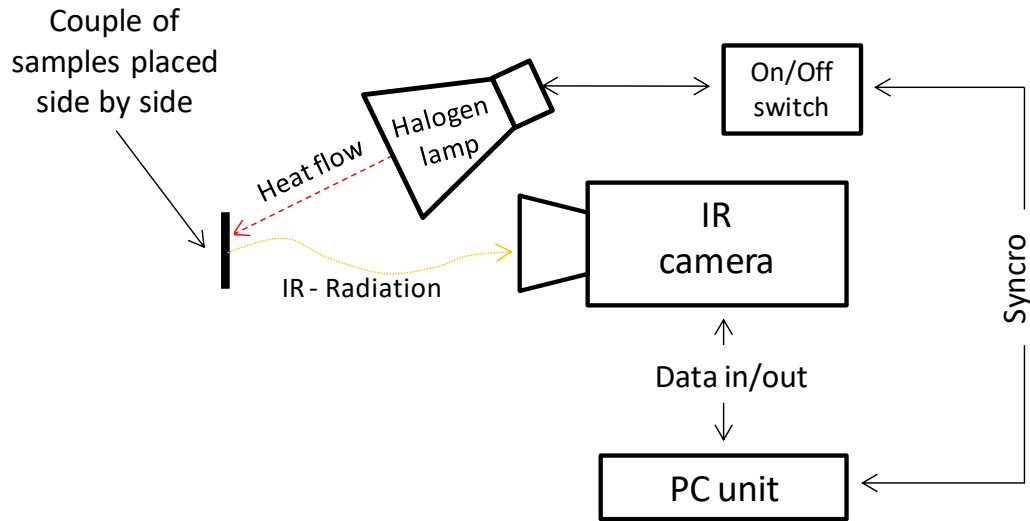
Figure 2. Experimental thermographic setup.

The thermographic analysis approach consists in the application of a heating and cooling cycle to the samples, in order to detect differences in the thermal response to the heat transfer transients [e.g., 39].

An halogen lamp, with the power of 1500 W, has been used as a heat source and is placed on the front side of the samples slightly tilted down as shown in the Figure 2. An Infrared-Camera is placed on the same side of the halogen lamp and focused on the sample surface to monitor the temperature distributions changes over the time, see specifications of the IR-Camera in Table 2. In Table 3 the main experimental parameters used for the thermographic setup are listed.

Table 2. Specification of the Ir-Camera

Thermocamera	
Brand	FLIR
Model	X6540sc
Sensor	Focal Plane array, InSb

Resolution (h×v)	640×512 pixels
Spectral response	1.5-5 μm
Lens (hfov × vfov)	MW 25 mm F/2.0 (21.74°×17.46°)
Noise (NETD)	20 mK

Table 3. Experimental parameter value used in the setup of the thermographic experiments.

Parameter setup	Value
Distance sample to IR camera	~430 mm
Distance halogen lamp to sample surface	~300 mm
Sample rate IR camera	10 Hz
Instantaneous Field Of View (IFOV)	0.19 mm
Integration time	1500 μs

For each experiment the IR-Camera collects the temperature evolution over the time in a region of interest of the sample, see Figures 3 (a) and 3 (b). The region of interest has the same dimension (of 16 mm x 32 mm) in all the performed analyses and includes a great percentage of the total frontal surface of the samples. Specimens are supported by a base that stays at a lower temperature and drains the heat making the lower part of the samples colder than the remaining surface, as can be seen in Figure 3 (b).
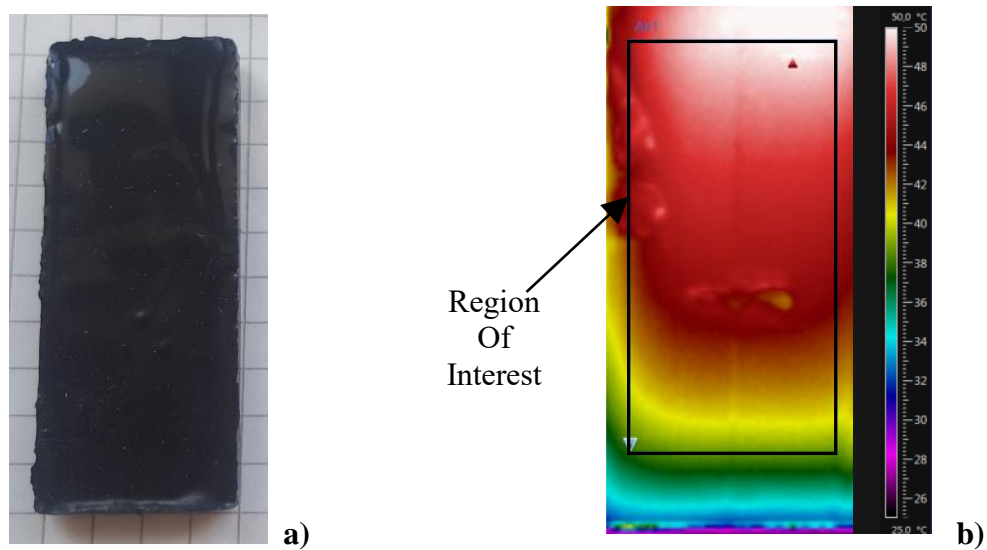
a)

b)

Region
Of
Interest

Figure 3. a) Sample, b) Acquired thermographic image of the sample with definition of the Region of

Interest (defined by a black line).

The thermal behaviour is obtained calculating the mean of the temperature values acquired over the

region of interest. In Figure 4 an example of the acquired thermal behaviour during the heating/cooling
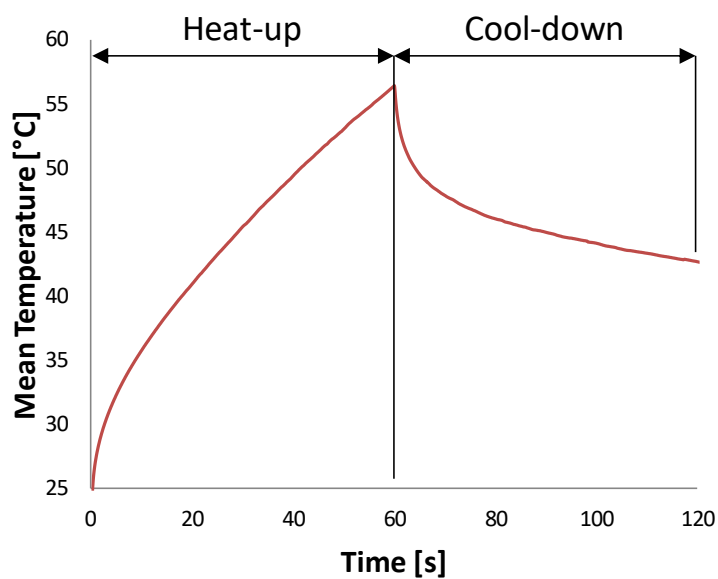
cycle is shown.

Figure 4. Example of heating/cooling cycle obtained monitoring the surface mean temperature of the sample.

As shown in Figure 4 the heat-up part of the cycle terminates when the surface mean temperature reaches the range of 55-60°C.

The reason why a temperature range is indicated, rather than a precise fixed value, is that the graphs, like the one in Figure 4, have been obtained with a post-process, after the acquisition in the laboratory has been completed. During the acquisition the operator refers to a local indicator to evaluate the sample temperature and uses this local temperature to interrupt the heating cycle. The differences between the local and global (average) temperature are the cause of this slight change in the maximum temperature reached in the tests. That said, there was no evidence that the trend could change by increasing or reducing the acquisition time and this proves the robustness of the results.

2.4 Material characterisation

In order to characterise the nanofiller dispersion and the microstructure of the nanocomposites, a Scanning Electron Microscopy (SEM) was used. Figures 5 show a view of the fracture face of a sample prepared with the vacuum planetary mixer, THINKY, and with MWCNTs at 5wt%. In Figures 5 (b) and 5 (c), which have a higher magnification than picture 5 (a), it is possible to identify a good dispersion of MWCNTs.
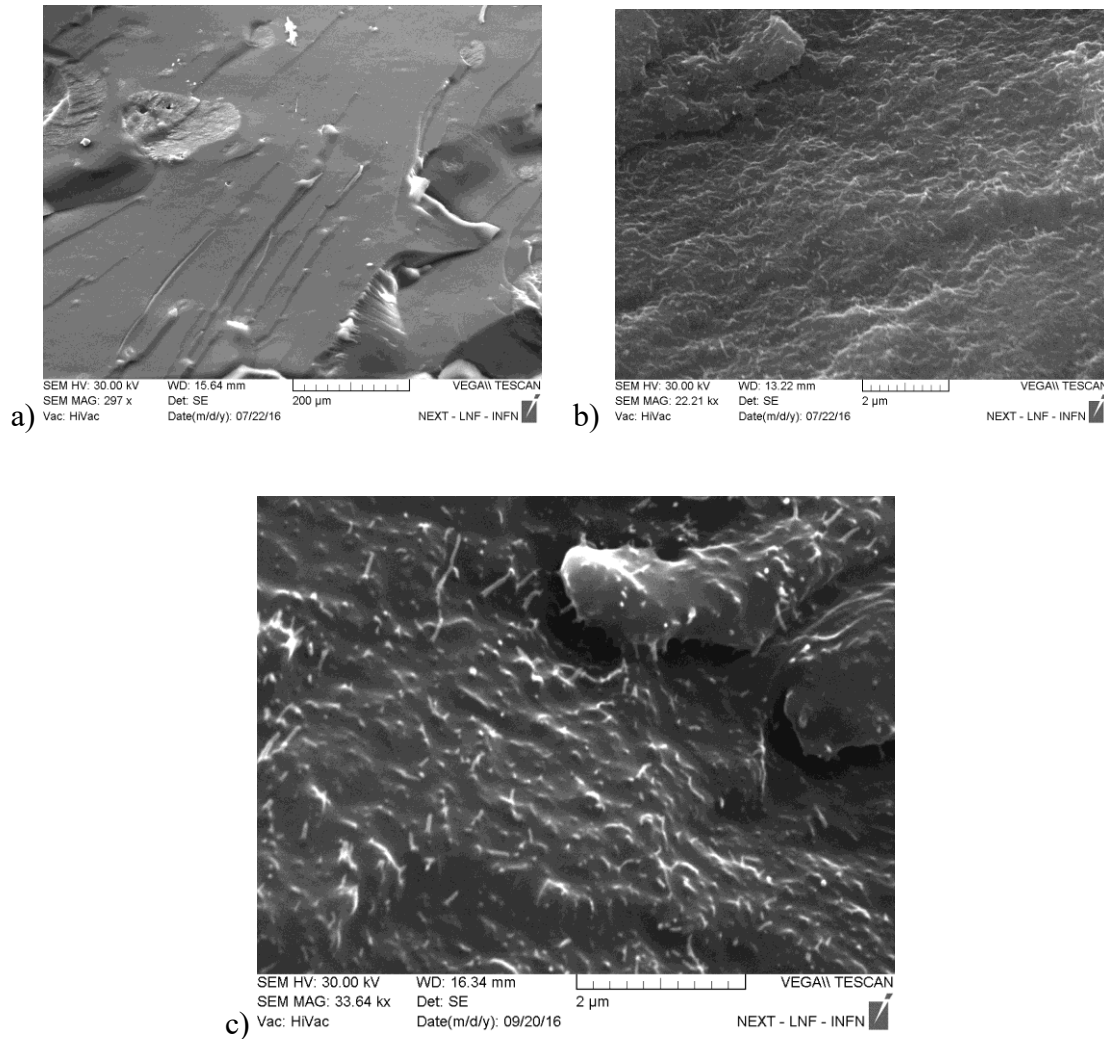
Figures 5. SEM images of the fracture face of a sample prepared by THINKY and with MWCNTs 30-50nm at 5wt%. In Figures 5 b) and 5 c) it is possible to identify a good dispersion of MWCNTs thanks to the higher magnification

Fig. 1 b and Fig 5 c were produced with the same magnification (2um scale), however, there is a distinct difference in the length of CNTs. In Fig.1 mostly 1-2 um long wires can be observed while in Fig. 5 it is hard to identify a tube longer than 500 nm. One might wonder whether CNTs break when processed to put them into the epoxy. However, it is simply due to the polydispersion of the CNTs length used as fillers in preparing the composite samples, which ranges between 0.5 micron and 200 micron.

Figures 6 shows a view of the fracture face of a sample prepared with the first procedure, HANDS, and with MWCNTs at 5wt%. In Figures 6 (a) and 6 (b) it is not so simple to identify MWCNTs, but it is possible to find several bubbles. In Figures 6 (c), which have a higher magnification than picture 6 (a) and 6 (b), it is possible to find MWCNTs in the resin, but they are not well dispersed, rather they are clearly aggregated in bundles.
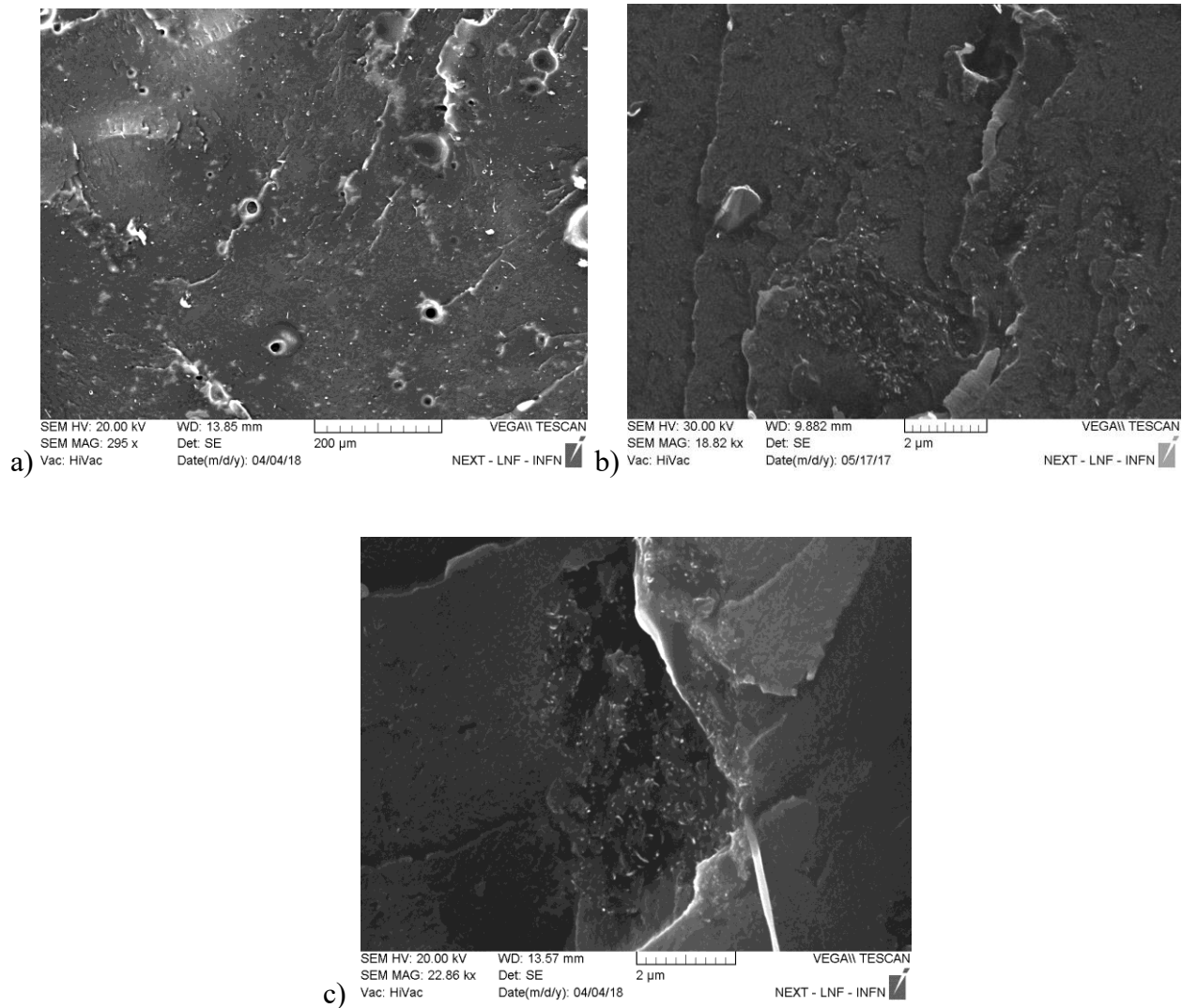

Figures 6. SEM images of the fracture face of a sample prepared by hand mixing, HANDS, and with MWCNTs at 5wt%. In a) and b) it is not so simple to detect MWCNTs, but it is possible to find several

air bubbles. In c) thanks to higher magnification it is possible to see MWCNTs in the resin aggregated in bundles.

3. Results

In order to validate the novel NDE technique, several couples of specimens with various volume fractions and diameter ranges of CNTs have been manufactured and tested. The NDE thermographic approach was then used to compare pairs of samples whose difference is represented only by the dispersion level of the MWCNTs into the epoxy matrix, which is much better in samples manufactured by THINKY, i.e. in the vacuum planetary mixer, in comparison to those produced by HANDS. What was found is a significant difference in the thermal response to the heat transfer transients, i.e. the pairs of specimens, with dissimilar level of dispersion, have clearly distinguishable thermographic outcomes.

Each comparison involves a pair of samples placed side by side at the same distance from the heat source, in order to guarantee the same level of irradiation for both. Four types of nanocomposites, characterized by volume fraction and diameter range of MWCNTs, were compared: 5 wt.% and 8-15 nm outer diameter range, 10 wt.% and 8-15 nm outer diameter range, 5 wt.% and 30-50 nm outer diameter range, 10 wt.% and 30-50 nm outer diameter range. Several specimens of each type, produced both with the first procedure and the second one, were used in this work. In Figures 7 a) to d), for each of the four combinations of volume fraction and diameter range of MWCNTs, it is presented a comparison between the thermal response of two samples characterized by the two different manufacturing techniques, and thus by different dispersion levels. The thermographic method used for acquiring the thermal behaviour of each sample during the heating/cooling cycle is described in the paragraph 2.3.

As specified in section 2.2, the samples have exactly the same thickness of 5 mm, but a further series of thermographic measurements has been recorded to investigate how a small change in thickness

can influence the results. After several comparisons between samples, which differ only in their thickness but have the same type of manufacture (THINKY or HANDS), same CNT diameter and same weight fraction of fillers, it is possible to state that the maximum average temperature recorded in the region of interest does not change due to variation in thickness up to 8%. What changes is the time needed to reach the same temperature, so there is a horizontal shift in time, a delay, for the thicker specimen with respect to a thinner one. This demonstrates the robustness of the method even when there are small variations in the thickness of the samples.
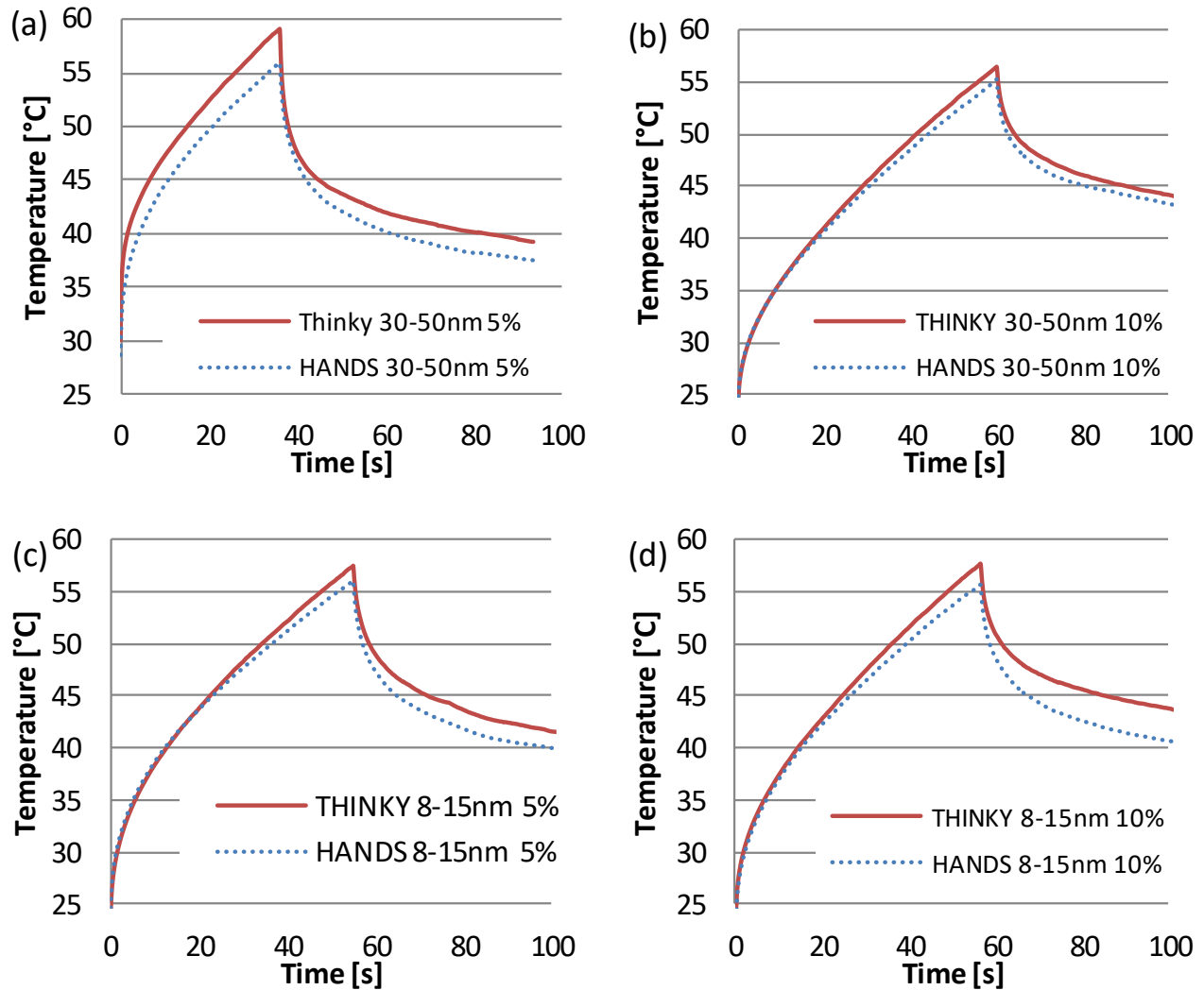
Figure 7. Comparisons between the thermal response of couple of samples characterized by the two different manufacturing techniques, and thus by different dispersion levels of MWCNTs into the resin. Four graphs for different wt.% and diameter range of MWCNTs are shown: a) 5 wt.% and 30-50 nm diameter range, b) 10 wt.% and 30-50 nm diameter range, c) 5 wt.% and 8-15 nm diameter range, d) 10 wt.% and 8-15 nm diameter range. In all graphs it is the mean temperature of the specimen surface which is plotted at the y axis, according to the thermographic method described in the paragraph 2.3.

Figures 8 a), for samples with 5 wt.% and 30-50 nm diameter range of MWCNTs, and 8 b), for samples with 10 wt.% and 8-15 nm diameter range of MWCNTs, report the thermographic images of a pair of samples, placed side by side, at the end of the heating phase. Both in Figures 8 a) and in 8 b) the sample manufactured by HANDS is on the left in the image, while the sample produced by THINKY is shown on the right. The images have been automatically subjected to a slight interpolation.
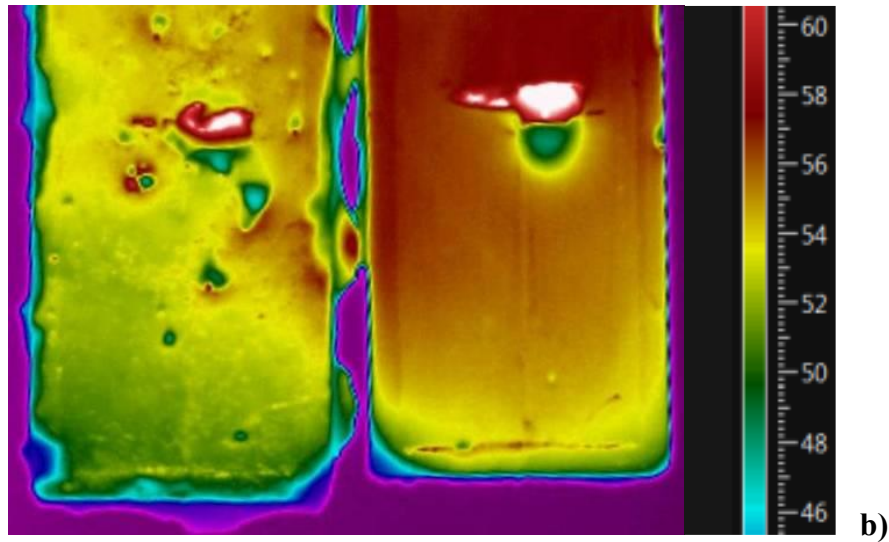

a)

b)
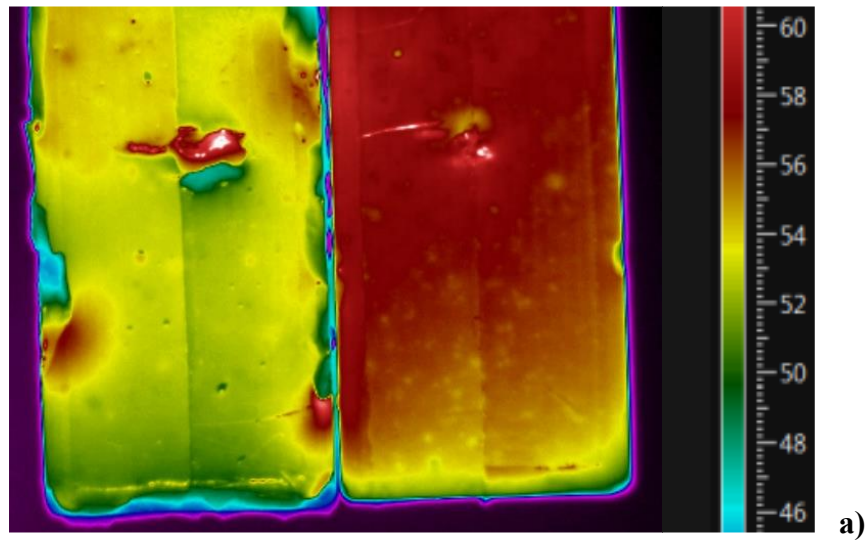
Figure 8. Thermograms of a pair of samples, placed side by side, at the end of the heating phase: a) for samples with 5 wt.% and 30-50 nm diameter range of MWCNTs, b) for samples with 10 wt.% and 8-15 nm diameter range of MWCNTs. In both thermograms a) and b) the sample manufactured by HANDS is on the left, while the sample produced by THINKY is on the right.

Figure 7 and 8 visibly show the effects of MWCNTs dispersion on the thermal response of the nanocomposites to the heat transfer transients. Samples produced by THINKY always reach higher temperature than those manufactured by HANDS when exposed to the same amount of heat flux on the surface. The maximum difference in the means of the temperatures acquired over the region of interest at the end of the heating phase varies between 1.5 °C and 3.5 °C. Considering that the Noise Equivalent Temperature Difference (NETD) of the thermocamera is equal to 20 mK, this result confirms that a correlation exists between the thermal behaviour of the nanocomposite and the level of dispersion of the CNTs inside it. In thermography a difference of 1.5 °C or higher is considered a clearly distinguishable outcome and can be used to identify consistently the thermal response of a material with respect to another. Moreover, we can state that the raising-up of the temperature in samples exposed to

the same heat flux, is faster for samples with a better dispersion level compared to those with a poor dispersion level.

Thus, the novel NDE technique can be used to check the quality, in terms of dispersion levels, of products made of nanocomposites based on epoxy and MWCNTs, in order to guarantee that the expected specifications are met. A reference product, which has the expected dispersion level and achieves the desired design performance, can be used to test the thermal behaviour of other products coming out of the production process and those with poor dispersion can be identified.

A clear understanding of the mechanism behind the effects of MWCNTs dispersion on the thermal response of the nanocomposites to the heat transfer transients can be easily provided taking into account the three following considerations.

Thermal conductivity of epoxy resin is almost two thousand times smaller than that of MWCNTs, thus their presence in the matrix, even in limited percentages, has dramatic effects on the thermal response of the resulting nanocomposites. For a fixed weight fraction of MWCNTs, a homogeneous dispersion maximizes the interface area between the MWCNTs and the matrix and, accordingly, the MWCNTs effects on the thermal response of the resulting nanocomposites is also maximized. Since an addition of 0.5 wt% MWCNT, for the same heating / cooling cycle, makes the maximum temperature recorded by a thermographic analysis of about 10 °C higher than in the case of pure epoxy resin, [eg 40], in a comparison between composites with different levels of dispersion the difference in the temperatures can't be higher than few degrees Celsius, which however in thermography represent a clearly distinguishable result.

The other central aspect that drives the physical phenomenon regards the thermal conductivity of individual MWCNTs, which is at least four times higher than the thermal conductivity within MWCNT bundles [27-29], as discussed in paragraph 2.1. Thus, in nanocomposites where a significant percentage

of MWCNTs is aggregated in bundles due to the poor dispersion, the temperatures recorded in a thermographic analysis, for the same heating/cooling cycle, are lower than for nanocomposites with good dispersion.

The third mechanism that explains the effects of MWCNTs dispersion on the thermal response of the nanocomposites is that the specific heat of individual MWCNTs is 33% lower than the specific heat of MWCNTs bundles [28]. Since the specific heat is the amount of heat per unit mass required to raise the temperature by one degree Celsius, a given volume fraction of MWCNTs bundles will require more heat to rise the temperature, with respect to the same volume fraction of homogenously dispersed individual MWCNTs.

A final consideration needs to be done regarding the air bubbles seen in the SEM image, Figure 6, for the samples manufactured by the procedure called HANDS. Since thermal conductivity of air is extremely small, around 0.0257 W/m K at 20 °C, the effect of the presence of air bubbles is to rise the temperatures detected by the infrared camera on the surface of the sample. Thus, if the effect of the air bubbles were dominant, then the temperatures recorded in samples produced by HANDS would have been higher than in those manufactured by THINKY, but this was not the case in any of the experiments. It follows that the effect of the air bubbles in samples produced by HANDS is of secondary importance, with respect to the dispersion levels of the MWCNTs.

4. Conclusions

An extensive use of CNTs enhanced polymer composites can be boosted by novel NDE techniques able to check the quality of the products made of these nanocomposites in order to guarantee that their specifications are met. It is well known in literature that the parameter that much more than others can affect the enhancing capabilities of the added nanoparticles is their dispersion. All the resulting physical properties of the CNTs based polymer composites depend strongly on level of dispersion of the CNTs

throughout the matrix. Here we have presented a novel NDE technique based on infrared thermography able to test the dispersion of the added nanoparticles in nanocomposites. Two different procedures were selected to prepare epoxy nanocomposites with dissimilar degree of nanoparticle dispersion. The novel NDE technique was then used to compare pairs of specimens whose only difference is represented by the dispersion level, which is much better in the samples manufactured by THINKY, a vacuum planetary mixer, compared to those produced by HANDS. We found a significant difference in the thermal response to the heat transfer transients, i.e. the pairs of specimens, with dissimilar level of dispersion, have clearly distinguishable thermographic outcomes. The raising up of the temperature in samples exposed to the same heat flux, is faster for those with a better level of dispersion, compared to those with a poor dispersion. Thus, the NDE technique can be used to identify consistently the thermal response of a material with respect to another. A reference product, which has the expected dispersion level and achieves the desired design performance, can be used to test the thermal behaviour of other products coming out of the production process and those with poor dispersion can be identified. The mechanisms behind the effects of MWCNTs dispersion on the thermal response of the nanocomposites to the heat transfer transients were identified: homogeneous dispersion maximizes the interface area between MWCNTs and resin, the thermal conductivity of individual MWCNTs is at least four times higher than the thermal conductivity within MWCNTs bundles, the specific heat of individual MWCNTs is one third smaller than the specific heat of MWCNTs bundles.

References

1. M. El Achaby, A. Qaiss , *Materials and Design*, **2013**, 44, 81.

2. G. Zamfirova, V. Gaydarov, F. Faraguna, E. Vidović, A. Jukić, *Colloids and Surfaces A: Physicochemical and Engineering Aspects*, **2016**, 510, 169.

3. J. Zhong, A. I. Isayev, X. Zhang, *European Polymer Journal*, **2016**, 80, 16.

4. D. Lai,Y. Wei, L. Zou, Y. Xu, H. Lu, *Progress in Natural Science: Materials International*, **2015**, 25, 445.

5. R. Blake, J.N. Coleman, M.T. Byrne, J.E. McCarthy, T.S. Perova, W.J. Blau, A. Fonseca, J.B. Nagy and Y.K. Gun'ko, *Journal of Materials Chemistry*, **2006**, 16, 4206.

6. H. Yazdani, B. E. Smith, K. Hatami, *Composites: Part A*, **2016**, 82, 65.

7. Q. Zhang, J. Wu, L. Gao, T. Liu,W. Zhong, G. Sui, G. Zheng, W. Fang, X. Yang, *Materials and Design*, **2016**, 94, 392.

8. E.Y. Choi, S.C. Roh, C.K. Kim, *Carbon*, **2014**, 72, 160.

9. J. Dong, Y. Fang, F. Gan, J. An, X. Zhao, Q. Zhang, *Composites Science and Technology*, **2016**, 135, 137.

10. A.A. Mamedov, N.A. Kotov, M. Prato, D.M. Guldi, J.P. Wicksted and A. Hirsch. *Nature Materials*, **2002**, 1, 190.

11. R. Haggenmueller, C. Guthy, J.R. Lukes, J.E. Fischer and K.I. Winey, *Macromolecules,* **2007**, 40, 2417.

12. W.T. Hong and N.H. Tai, *Diamond & Related Materials*, **2008**, 17, 1577.

13. C. Guthy, F. Du, S. Brand, K.I. Winey and J.E. Fischer, *J Heat Transfer*, **2007**, 129, 1096.

14. K. Yang K, M. Gu, Y. Guo, X. Pan and G. Mu, *Carbon*, **2009**, 47, 1723.

15. P.C. Ma, A. N. Siddiqui, G. Marom and J.K. Kim, *Composites: Part A*, **2010**, 41, 1345.

16. J. Gorrasi, M. Sarno, A. Di Bartolomeo, D. Sannino, P. Ciambelli and V. Vittoria, *Journal of Polymer Science Part B: Polymer Physics*, **2007**, 45, 597.

17. F.H. Gojny, M.H.G. Wichmann, B. Fiedler, I. Kinloch, W. Bauhofer, A.H. Windle and K. Schulte, *Polymer*, **2006**, 47, 2036.

18. Y. Zeng, Z. Ying, J. Du and H.M. Cheng, *The Journal of Physical Chemistry C*, **2007**, 111, 13945.

19. I. Singh, P.K. Bhatnagar, P.C. Mathur, I. Kaur, L.M. Bharadwaj and R. Pandey, *Carbon*, **2008**, 46,1141.

20. N. He, Y. Chen, J. Bai, J. Wang, W.J. Blau, J. Zhu, *The Journal of Physical Chemistry C*, **2009**, 113, 13029.

21. M. Baibarac and P. Gómez-Romero, *Journal for Nanoscience and Nanotechnology*, **2006**, 6, 1.

22. J. Wang and W.J. Blau, *The Journal of Physical Chemistry C*, **2008**, 112, 2298.

23. E. Ivanov, H. Velichkova, R. Kotsilkova, S. Bistarelli, A. Cataldo, F. Micciulla and S. Bellucci. *Applied Rheology*, **2017**, 27, 12.

24. V. Levin, Y. Petronyuk, E. Morokov, L. Chernozatonskii, P. Kuzhir, V. Fierro, ... and S. Bellucci, *physica status solidi (b)*, **2016**, 253, 1952.

25. V. Levin, E. Morokov, Y. Petronyuk, A. Cataldo, S. Bistarelli, F. Micciulla and S. Bellucci, *Polymer Engineering & Science*, **2017**, 57, 697

26. S. Berber, Y-K Kwon, D. Tomanek, *Phys. Rev. Lett.*, **2000**, 84, 4613–6.

27. A.E. Aliev, M.H. Lima, E.M. Silverman, R.H. Baughman, *Nanotechnology*, **2010**, 21, 035709.

28. N.R. Pradhan, H. Duan, J. Liang, G.S. Iannacchione, *Nanotechnology*, **2009**, 20, 245705.

29. L. Shi, D. Li, C. Yu, W. Jang, D. Kim, Z. Yao, P. Kim, A Majumdar, *J. Heat Transfer*, **2003**, 125, 881.

30. S. Bellucci; C. Balasubramanian; F. Micciulla; G. Rinaldi, *Journal of Experimental Nanoscience*, **2007**, 2, 193.

31. S Bellucci, C Balasubramanian, G De Bellis, F Micciulla, G Rinaldi, *Macromolecular symposia,* **2008**, 263, 21.

32. S Bellucci, L Coderoni, F Micciulla, G Rinaldi, I Sacco, *Journal of nanoscience and nanotechnology*, **2011**, 11, 9110.

33. S Bellucci, L Coderoni, F Micciulla, G Rinaldi, I Sacco, *Nanoscience and Nanotechnology Letters*, **2011**, 3, 826.

34. P Kuzhir, A Paddubskaya, D Bychanok, A Nemilentsau, M ShubaA Plusch, S Maksimenko, S Bellucci, L Coderoni, F Micciulla, I Sacco, G Rinaldi, J Macutkevic, D Seliuta, G Valusis, J Banys, *Thin Solid Films*, **2011**, 519, 4114.

35. PP Kuzhir, AG Paddubskaya, MV Shuba, SA Maksimenko, A Celzard, V Fierro, G Amaral-Labat, A Pizzi, G Valušis, J Macutkevic, M Ivanov, J Banys, S Bistarelli, A Cataldo, M Mastrucci, Micciulla, I Sacco, E Stefanutti, S Bellucci, *Journal of Nanophotonics*, **2012**, 6, 061715.

36. P Kuzhir, A Paddubskaya, A Plyushch, N Volynets, S Maksimenko, J Macutkevic, I Kranauskaite, J Banys, E Ivanov, R Kotsilkova, A Celzard, V Fierro, J Zicans, T Ivanova, R Merijs Meri, I Bochkov, A Cataldo, F Micciulla, S Bellucci, Ph Lambin, *Journal of Applied Physics*, **2013**, 114, 164304.

37. J Macutkevic, PP Kuzhir, AG Paddubskaya, J Banys, SA Maksimenko, E Stefanutti, F Micciulla, S Bellucci, *Journal of Nanophotonics*, **2013**, 7, 073593.

38. Joseph H. Koo, *Fundamentals, Properties, and Applications of Polymer Nanocomposites*, Cambridge University Press, December **2016**

39. G Pitarresi, *SDHM Structural Durability and Health Monitoring*, **2012**, 8, 149.

40. I. Taraghi, A. Fereidoon, *Composites Part B*, **2016**, 103, 51.